Conformational analysis of josamycin, a 16-membered macrolide free in solution and bound to bacterial ribosomes

Josyane Gharbi-Benarous,[ab] Nathalie Evrard-Todeschi,[a] Patrick Ladam,[a] Gildas Bertho,[a] Marcel Delaforge[a] and Jean-Pierre Girault*[a]

[a] *Université René Descartes-Paris V, Laboratoire de Chimie et Biochimie Pharmacologiques et Toxicologiques (URA 400 CNRS), 45 rue des Saint-Pères, 75270 Paris Cedex 06, France*
[b] *Université Denis Diderot-Paris VII, UFR Chimie, 2 Place Jussieu, F-75251 Paris Cedex 05, France*

Received (in Cambridge) 27th October 1998, Accepted 18th January 1999

The potent 14-membered macrolide antibiotics displayed a strong NMR response in the TRNOESY experiments whereas their metabolites which do not retain antimicrobial activity gave essentially blank TRNOESY spectra. These TRNOESY experiments are here extended to a macrolide (josamycin) belonging to the 16-atom macrolide class in order to compare responses according to the macrocycle size. Analysis of transferred nuclear Overhauser effect (TRNOE) experiments resulted in a set of constraints for all proton pairs. These constraints were used in structure determination procedures based on molecular modelling to obtain a bound structure compatible with the experimental NMR data. This study allowed us to identify the binding structure at the ribosome for the active 16-membered macrolide. The different conformations existing in solution for this antibiotic in the free state will be compared and correlated with the binding conformation at the ribosome obtained with TRNOE experiments so as to establish a structure–activity relationship. The comparative results indicate that one conformation (called **S3**) pre-existing in the conformational equilibrium of macrocycle in solution and close to the major one **S5**, is preferred in the bound state.

Introduction

Macrolide antibiotics play a therapeutically important role, particularly with the emergence of new pathogens. Structural differences are related to the size of the lactone ring and to the number and nature (neutral or basic) of the sugars. Natural macrolides are classified (Fig. 1) according to the size of the lactone ring (12, 14, 15 or 16 atoms).[1] The macrolide antibiotic family (14-, 15- and 16-membered ring derivatives) shows a wide range of characteristics (antibacterial spectrum, side-effects and bioavailability). The most commonly used macrolides are erythromycin and josamycin (Fig. 2).

The search for macrolides active against MLS-resistant strains (MLS = Macrolides–Lincosamides–Streptogramines) has become a major goal, together with retaining the overall profile of the macrolides in terms of stability, tolerance and pharmacokinetics. Semisynthetic molecules have recently been developed from erythromycin A; new compounds containing a 14-membered lactone ring with chemical modifications to enhance acid stability[2,3] and prevent anhydro formation[4] include roxithromycin and clarithromycin (Fig. 2). Josamycin is a remarkably stable macrolide in contrast with the acid degradation of erythromycin.[5]

The 16-membered ring macrolide antibiotics constitute an important clinically useful series of naturally occurring compounds within the macrolide class of antibiotics, as they show some advantages over 14-membered ring compounds (gastrointestinal tolerance and activity against strains expressing resistance of the inducible type). Therapeutic interest in this antibiotic class picked up with emergence of new pathogens such as *Legionella* spp. They represent the main alternative in cases of allergy to β-lactam antibiotics and tetracycline.[2]

Their rather complex molecular structures, with the characteristic diene and polyoxygenated systems, may be regarded as

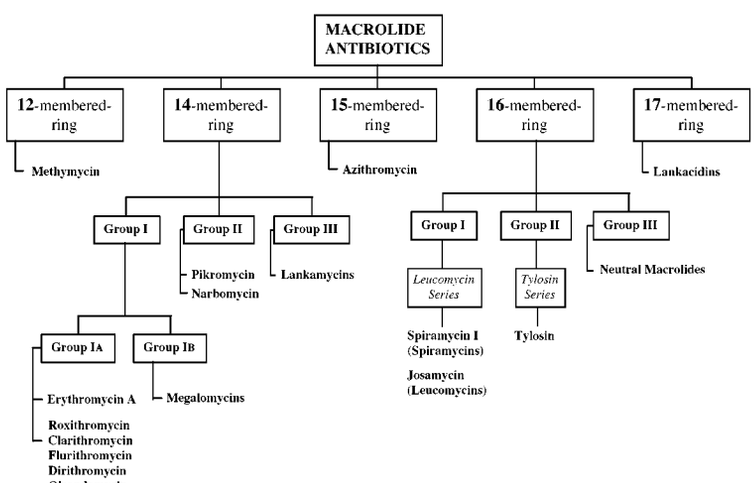

Fig. 1 Classification of macrolide antibiotics.

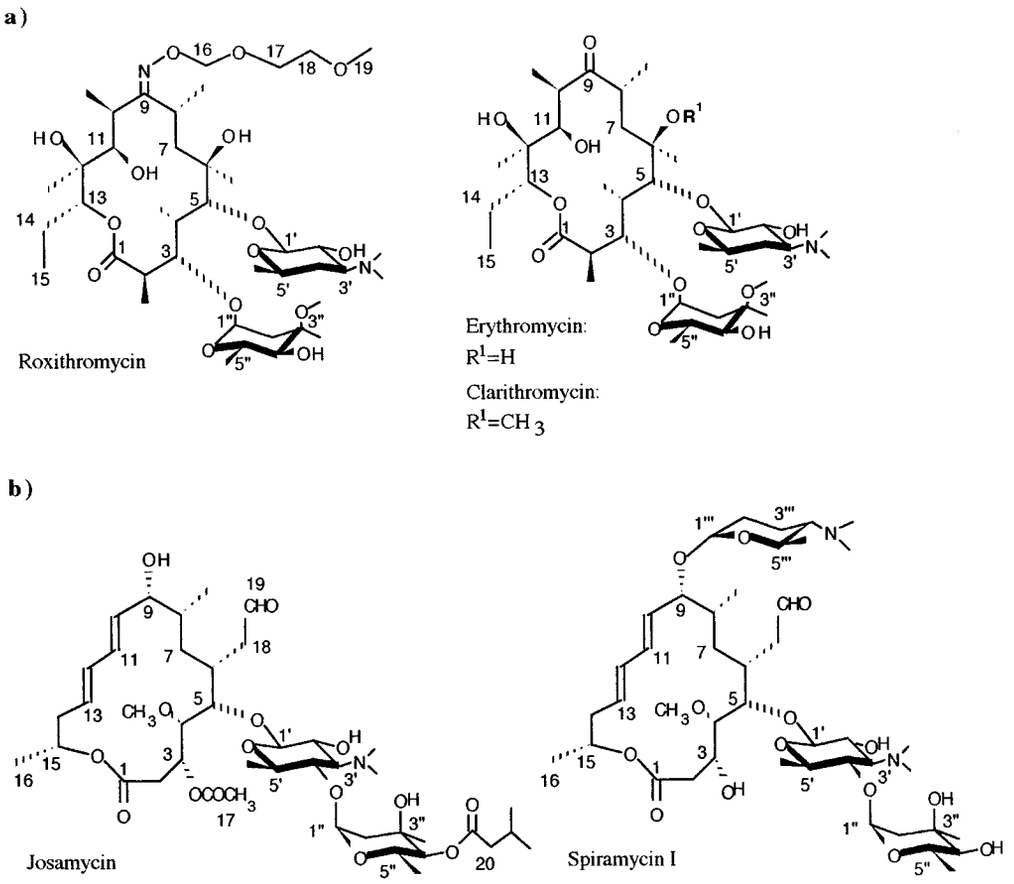

Fig. 2 Chemical structures of the a) 14-membered ring macrolides: erythromycin, clarithromycin and roxithromycin, and the b) 16-membered ring macrolides: josamycin and spiramycin I.

structurally intermediate between the lower ring size macrolide antibiotics (*e.g.*, erythromycin) and the higher size polyene macrolides (*e.g.*, amphotericin). Macrocyclic lactones are generally substituted by two non-classical sugar residues *via* glycosidic bonds. In the 14-atom series, these residues are bound individually by their anomeric carbon atoms, while in the 16-atom series the sugar moiety is usually a disaccharide, covalently bound to the lactone ring by the anomeric carbon of a dimethylamino sugar (Fig. 2). Maximum activity requires both sugars and neither the free sugars nor the free lactone are active.

The compound studied here is josamycin (Fig. 2b) since it has a similar antibacterial spectrum and its activity *in vivo* is comparable (with minor exceptions) to erythromycin A. A first partial structure was reported by Watanabe *et al.*[6] and the total structure was proposed by Hata *et al.*[7] in 1967 while the X-ray crystal structure obtained by Hiramatsu *et al.* corresponds to that of demycarosyl josamycin.[8] The primary goal of this work was to determine the overall solution conformation of josamycin. This was accomplished by obtaining information about dihedral angles from the vicinal coupling constant data, by acquiring the spatial proximity information from nuclear Overhauser effect data and through the use of molecular modelling by mechanics and dynamics calculations. It is first necessary to assign the ^{1}H and ^{13}C NMR spectra of the drug.

In this article, we will try also to shed light on the conformation of josamycin bound to bacterial ribosomes, beyond what is already known on the mechanism of action of the 16-membered macrolides. Macrolide antibiotics like erythromycin A and roxithromycin inhibit protein biosynthesis in the elongation step by binding to the 50S bacterial ribosome. There appear to be two stages to this binding: a weak interaction which can be detected by NMR spectroscopy,[9,10] and a stronger interaction ($K_d = 10^{-7}$–10^{-9} M)[11–13] detected by equilibrium dialysis and related methods. Taking advantage of the exchange between bound and free macrolide antibiotics, we have previously developed a study on the macrolide–ribosome weak interactions with *E. coli* ribosomes of the 14-membered ring class [erythromycin, roxithromycin, their metabolites and their methylated derivatives (*e.g.*, clarithromycin)] using line broadening and transferred NOESY (TRNOESY) experiments.[9,14–16] TRNOE NMR experiments were proved to be efficient for the location and detection of weak interactions due to ribosomal activity, providing a means to study the relationship between the conformation of molecules when interacting and their activity.

Earlier work[17] on the strong interactions ($K_d = 10^{-7}$ to 10^{-9} M) performed with the 16-membered macrolide, spiramycin I (Fig. 2) has given rise to the description of the macrolides as translocation inhibitors (erythromycin series) or peptidyltransferase inhibitors (spiramycin series) and to the conclusion that spiramycin and erythromycin bind to different sites. Thus, in this study TRNOESY experiments were extended to the macrolide josamycin (group I, leucomycin series) belonging to the 16-membered macrolide class (Fig. 1) in order to compare the weak interaction responses according to the macrocycle size. It was noticed that josamycin generally showed a slightly lower affinity for the 70S ribosome target than did erythromycin,[18] but displayed significantly good overall antibiotic activity. In order to compare the behaviour of josamycin, its conformation when weakly bound to bacterial ribosomes was determined. Moreover, in the ribosome complex, from the constraints of the different TRNOEs observed in D_2O solvent, we propose to analyse whether the active molecules belonging to the 14- and 16-membered macrolide classes present a shared bound region or if the conformations when weakly bound to bacterial ribosomes vary.

Table 1 Notation for conformer designations defined as **M1**, **M2**, **M3**, **D1**, **D2**, **D3**, **D4**, **C1**, **C2**, **C3**, **C4** and **C5**

	Macrocycle conformations		
Torsion angles	**M1**	**M2**	**M3**
H(2pR), H(3)	175°	−85°	−70°
H(4), H(5)	175°	130°	−70°
H(6), H(7pR)	180°	170°	175°
H(9), H(10)	−150°	−145°	180°

	Mycaminose conformations			
	D1	**D2**	**D3**	**D4**
Ψ_1 [H(5), C(1′)]	10–15°	25°	(−15)–(−40)°	15°
Ψ_2 [C(5), H(1′)]	45–55°	50°	(−25)–(−10)°	150°

	Mycarose conformations				
	C1	**C2**	**C3**	**C4**	**C5**
Ψ_3 [H(4′), C(1″)]	170°	−160°	10–15°	−20°	50°
Ψ_4 [C(4′), H(1″)]	10–25°	55°	35–40°	−10°	75°

The macrolide antibiotics have been shown to affect hepatic metabolic enzymes, especially cytochrome P-450, as the dimethylamino function of the desosamine sugar is able to bind to the heminic iron of the cytochrome P-450 and to generate cytochrome P-450–nitroso metabolite complexes.[19] The formation of this complex is probably responsible for interference with the metabolism of other drugs[20] for time-dependent inhibition and induction of P-450s by erythromycin, phenomena that can lead to life-threatening drug–drug interactions.[3] 14-Membered drugs are different in their effects, roxithromycin weakly induces hepatic cytochrome P-450 while erythromycin has higher interaction properties with the cytochrome P-450 system. The interest of josamycin lies in its very low toxicity in comparison with erythromycin. Josamycin does not form a complex with cytochrome P-450 and has the advantage of not having any side effects.[20] Thus, it is often used for children.[21] The structural modifications which affect the formation of the inhibitory complex appear to be related to the addition of a sugar ring (mycarose) at the 4′-position of the mycaminose independent of the modification of the macrocycle molecular weight. Only the antibiotics containing the aminosugars (desosamine and mycaminose) were able to give induction of cytochrome P-450 and formation of an inhibitory cytochrome P-450–iron–nitrosoalkane metabolite complex. A structural factor is important for an antibiotic to lead to such effects: the presence of a non-hindered readily accessible *N*-dimethylamino group.[22]

16-Membered antibiotics such as josamycin and spiramycin, where one OH group of the mycosamine moiety bearing the mycarosyl moiety is replaced by a considerably more bulky *O*-sugar group, are completely unable to form the RNO complex. Accordingly, desmycarosyl–josamycin, which is derived from josamycin by hydrolysis of the *O*-sugar group (mycarose) to give a face OH group, becomes able to form this complex.[22]

Results and discussion

1. Structural characteristics of the free ligand, josamycin

As shown in Fig. 2, josamycin consists of three moieties, which are a 16-membered lactone, mycaminose and mycarose. The structural characteristics of josamycin include the presence of a hydroxy group at the C(9), an *O*-acetyl group at the 3-position of the lactone and an *O*-isovaleryl ester group on mycarose. The basic 16-membered macrolides are characterised by the presence of a formylmethyl group on the lactone ring. Considerable interest has been focused on the role of the formyl group. From the correlation between the structure and the biological activity of 16-membered ring macrolides, it has been shown that this functional group is important for the activity.[23]

The notations used for conformer designations for the macrocycle and sugar moieties are **M**, **D** and **C**, respectively, and Table 1 describes some of their characteristics. Experimental NMR and MD data are discussed with regard to these conformers, shown in Figs. 3–5.

The crystal structure of demycarosyl–josamycin obtained by X-ray diffraction revealed an interesting feature of the josamycin aglycone (**M1**) with the mycaminose sugar (**D1**) oriented perpendicular to the macrocyclic lactone ring.[24] The aglycone is

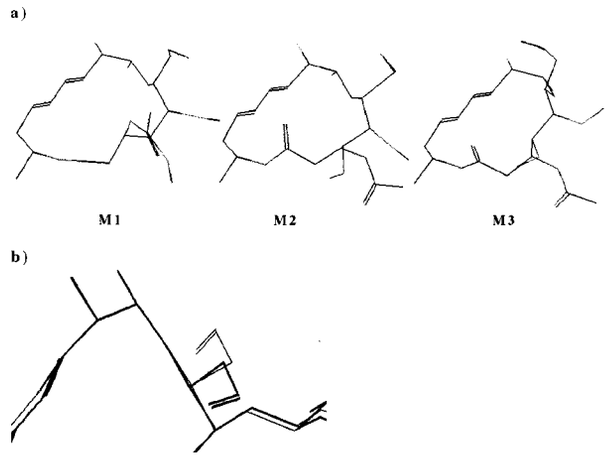

Fig. 3 a) The two conformations, **M1** with the H(3) proton 'folded-in' and the 3-*O*-acetyl group in a position 'up' above the macrocycle and **M2** with this group in an 'exo' orientation. A 'folded in' orientation of the H(3) proton in **M1**: H(2pS) and H(3) are either *gauche* (+60°) in **M1** or *trans* (170°) in **M2** and **M3**, while H(4) and H(5) are either *trans* (175°) in **M1** or *eclipsed* (+130°) in **M2** and *gauche* (+75°) in **M3**, respectively. b) The formyl group is in a major parallel position [$\varphi_{H6H18pS} = 180°$] with respect to the macrocycle. In molecular modelling calculations, an internal rotation occurred around the C(6)–C(18) bond leading to a minor perpendicular position [$\varphi_{H6H18pS} = 70°$].

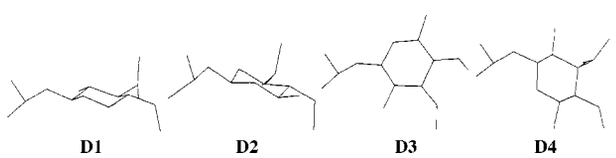

Fig. 4 Conformations of the mycaminose sugar ring following its orientation with respect to the lactone ring and the glycosidic dihedral angles, two orientations are perpendicular to the macrocycle **D1** (Ψ_1, 10°, Ψ_2, 50°) and **D2** (Ψ_1, 25°, Ψ_2, 50°) which is induced by the **M2** conformer; in the **D4** (Ψ_1, 15°, Ψ_2, 150°) position, the mycaminose sugar is coplanar to the macrocycle with a 'turn back' of 180° relative to the orientation **D3** (Ψ_1, −15°, −40°; Ψ_2, −25°, −10°).

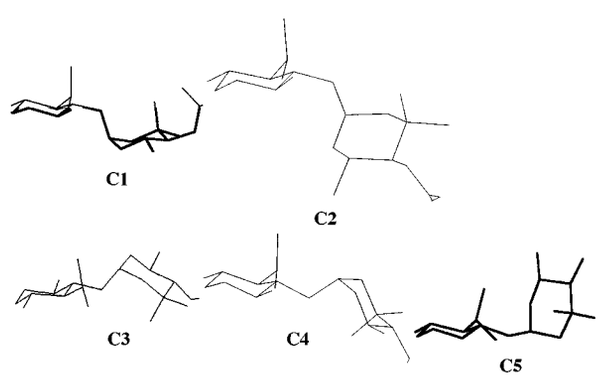

Fig. 5 The mycarose sugar adopts either conformation **C1** or **C2** ($\Psi_{H4'C1''} \approx 170°$) with a 'down' perpendicular glycosidic bond or conformations **C3**–**C5** ($\Psi_{H4'C1''} \approx \pm 40°$) with an 'up' perpendicular glycosidic bond.

Table 2 ^{1}H and ^{13}C NMR spectra of josamycin in D_2O and D_2O–DMSO (20 : 80) buffered solutions

	D_2O (0.5 mM, pH 7.6)			D_2O–DMSO (20 : 80, 4 mM)[a]		
Site	δ_H	δ_C	$J_{^1H,\ ^1H}$	δ_H	δ_C	$J_{^1H,\ ^1H}$
1	—		—	—	170.7	—
2a	2.63	27.9	13.5; 1.0	2.42	36.6	1.0; 11.5
2b	2.77	27.9	13.5; 11.4	2.57	36.6	11.2; 11.5
3	5.14		11.4; 1.5; 1.0	5.01	68.8	11.2; 1.0; 1.0
4	3.67	86.0	9.5; 1.5	3.32	83.9	9.2; 1.0
4-OMe	3.59		—	3.46	61.7	—
5	3.85	78.4	9.5; 1.0	3.71	75.6	9.2; 1.0
6	2.08		1.0; 11.4; 2.0; 12.3; 3.3	2.00	28.4	11.0; 13.5; 4.5; 1.0; 1.0
7a	1.12		14.5; 3.3; 10.3	0.93	29.8	13.5; 4.5; [b]
7b	1.52		14.5; 12.3; 3.4	1.42	29.8	13.5; 3.4; 3.5
8	1.96		4.0; 4.0; 3.4; 10.3	1.77	34.0	3.3; 6.5; 3.4; [b]
8-Me	1.01	16.5	4.0	0.93	15.1	6.5
9	4.09		9.8; 4.0	3.82	72.0	9.5; 3.3
10	5.83		9.8; 15.0	5.60	129.5	9.5; 15.0
11	6.50		10.5; 15.0	6.41	133.4	15.0; 10.5
12	6.26		10.5; 15.0	6.11	132.4	10.5; 14.6
13	5.71		15.0; 13.0; 4.3	5.64	131.1	14.6; 3.4; 10.3
14a	2.30		11.8; 12.5; 4.3	2.16	25.7	13.5; 10.3; 11.3
14b	2.60		11.8; 2.2; 11.0	2.52	25.7	13.5; 4.0; 3.4
15	4.90		6.4; 2.2; 12.5	4.91	70.5	6.1; 4.0; 11.3
16-Me	1.35		6.4	1.25	20.4	6.1
17	—		—	—	170.4	—
17-Me	2.2		—	2.15	21.2	—
18a	2.98		18.8; 11.4; 1.0	2.80	42.0	1.0; 19.0; 11.0
18b	2.58		18.8; 2.0; 1.0	2.34	42.0	1.0; 19.0; 1.0
19	9.67		1.0; 1.0	8.45	204.0	1.0; 1.0
20	2.47		4.8; 7.5	2.32	42.8	[b]; 7.0
20-CO_2	—		—	—	172.6	—
21	2.17		4.8; 6.8	2.05	25.4	6.6; 7.0
21-Me	1.02	24.3	6.8	0.97	22.3	6.6
1′	4.54	104.8	7.5	4.36	103.3	7.5
2′	3.75	72.1	7.5; 11.2	3.42	69.5	7.5; 11.0
3′	3.18		11.2; [b]	2.47	68.7	11.0; 9.5
3′-$N(Me)_2$	2.90	44.3		2.44	42.1	
4′	3.65		9.0; [b]	3.14	76.3	9.5; 9.5
5′	3.57		6.2; 9.0	3.20	71.7	5.9; 9.5
5′-Me	1.31		6.2	1.15	18.6	5.9
1″	5.33	98.9	1.9; 1.0	5.06	96.4	3.0; 1.0
2″-*eq*	2.12		[b]; 1.0	1.91	41.5	1.0; 14.5
2″-*ax*	2.12		[b]; 1.9	1.87	41.5	3.0; 14.5
3″	—		—	—	69.1	—
3″-Me	1.23	27.5	—	1.01	25.3	—
4″	4.76		10.0	4.48	77.2	10.3
5″	4.28	66.8	10.0; 6.2	4.38	62.7	10.3; 6.1
5″-Me	1.27		6.2	1.08	17.9	6.1

[a] Chemical shifts and coupling constants are determined in D_2O (buffered pH, 7.6)–DMSO (20 : 80) solution. [b] Undetermined because overlapping.

composed of a 16-membered lactone ring with a conjugated diene system and its seven substituents, *i.e.*, a methoxy, an acetyl, a formylmethyl, two methyl and two hydroxy groups. When viewed along the normal of the ring plane, the ring appears to be almost a rectangle. The diene part is incorporated into the longer side of the rectangle form keeping six of the ring carbon atoms zig-zag in a plane. The main difference from erythromycin or roxithromycin is that the conformations of the bonds C(1)–C(2), C(2)–C(3), C(3)–C(4), C(4)–C(5), are respectively *gauche*, *trans*, *trans*, *gauche* while in the 14-membered lactone ring, they should be respectively *gauche*, *gauche*, *trans*, *gauche*. Similarly to the diene region C(9)–C(14), the C(1)–C(5) atoms lie in a plane with the C=O(1) *trans* bond. The orientation of the acetyl group attached to the C(3) from the macro-ring plane is on the same side as C=O(1). It can also be seen that the sugar component, mycaminose (or 4′-hydroxy desosamine), is connected to the C(5) of the macro ring through a β-glycosidic linkage and its ring is perpendicular to the macro-ring plane.

This paper deals with the relationship between the biological activity and the conformations in solution which were obtained during structural studies on josamycin. To facilitate NMR studies of the binding of josamycin to bacterial ribosomes, the assignments of its ^{1}H and ^{13}C NMR spectra were required.

1.1 NMR spectroscopy. Initially, the solution of josamycin at pH 7.6 was used to obtain ^{1}H NOESY at 500 MHz. The assignments have been made using 1D ^{1}H and ^{13}C (^{1}H decoupled and DEPT-135)[25] spectra, 2D homonuclear double quantum (COSY) spectra, heteronuclear multiple bond correlation (HMBC) spectra[26] and heteronuclear multiple quantum correlation (HMQC) spectra.[27–29] ^{13}C assignments were then derived from ^{1}H–^{13}C correlations including long-range INEPT experiments.[30]

Josamycin is poorly soluble in aqueous buffers (1.5 mM). As it was not possible to obtain useful ^{1}H–^{13}C correlation spectra in D_2O solution, D_2O buffer–DMSO-d_6 (20 : 80) solutions (4 mM) were used. DMSO was used for these experiments because it showed an increased solubility of josamycin when compared with buffered D_2O solvent. The ^{1}H and ^{13}C NMR chemical shifts and coupling constants values for josamycin in buffered D_2O and D_2O–DMSO (20 : 80) solution are listed in Table 2.

1.1.1 Assignments of the ^{1}H, ^{13}C NMR signals. The 500 MHz ^{1}H NMR spectrum of josamycin in buffered D_2O solution at

25 °C, is shown in Fig. 6. The TOCSY spectrum was used to distinguish the spin groups 2a-2b-3-4-5-6, 6-18a-18b-19, 7a-7b-8-(CH_3-8), 9-10-11-12-13, 13-14a-14b-15-16, 20-21-(CH_3-21), 1′-2′-3′-4′-5′-(CH_3-5′), 1″-2″a-2″b, 4″-5″-(CH_3-5″) and the COSY spectrum was used to confirm the assignments of the hydrogen resonances within each spin group. The singlet at δ 2.90 corresponding to 3′-$N(CH_3)_2$ was assigned by inspection. The chemical shifts of the *N*,*N*-dimethyl protons will depend on the state of ionisation of that group.[31] One observes, in D_2O solution, that the amino group signal of josamycin at 2.90 ppm is similar to the resonance of the methyl in the protonated form.

^{13}C, DEPT-135 and ^1H–^{13}C correlation spectra (HMQC and HMBC) were obtained using the D_2O buffer–DMSO-d_6 (20 : 80) solution (4 mM). The DEPT-135 and ^1H–^{13}C correlation spectra were then used to assign the ^{13}C signals corresponding to the ^1H spin groups already assigned. The quaternary ^{13}C signals, the isolated *C*-methyl groups and the 4-*O*-methyl remained to be assigned. C(1)O, C(17)O and C(20)O (δ 170.7, 170.4 and 172.6) were assigned using the ^1H–^{13}C correlation HMBC spectra. H(4″) showed a cross-peak to a quaternary carbon signal at δ 69.1, which was assigned to C(3″). This, in turn, gave a cross-peak to δ_H 1.01, which was assigned to CH_3(3″). C(4) showed cross-peaks, to the methyl groups at δ_H 3.59 in D_2O and 3.46 in D_2O buffer–DMSO-d_6 (20 : 80). This signal was assigned to OCH_3(4), and the corresponding ^{13}C assignments were deduced from the ^1H–^{13}C spectrum. HMQC and HMBC spectra completed the assignments of the diene system and the three 3-, 6-, 4′-chains in D_2O buffer–DMSO-d_6 (20 : 80) solution and no significant changes in chemical shifts were observed throughout the chains except for the formyl group.

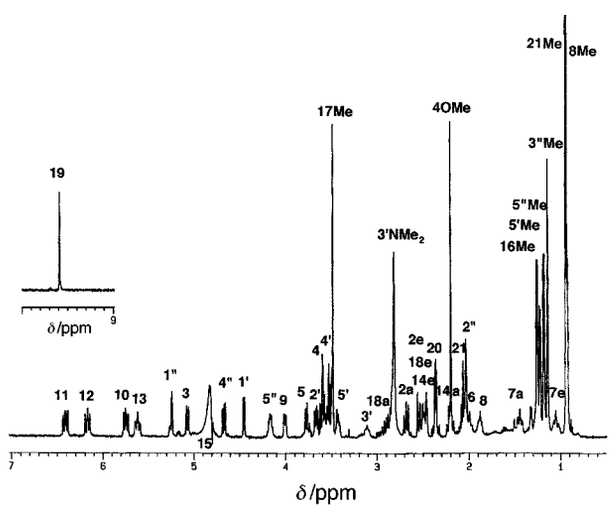

Fig. 6 500 MHz proton spectrum of a 1 mM solution of josamycin in buffered D_2O at 25 °C. Selected signals are identified.

The complete assignment of the ^1H spectrum in D_2O buffer–DMSO-d_6 (20 : 80) solution was useful to resolve any ambiguities for assignments in buffered D_2O. The poor solubility of josamycin in aqueous buffer made ^{13}C detected 2D experiments difficult.

1.1.2 Homonuclear $^3J_{^1H-^1H}$ and heteronuclear $^3J_{^{13}C-^1H}$ coupling constants. The determination of $^3J_{H,H}$ vicinal proton–proton coupling constants shown in Table 3 was used to predict the conformational analysis of the flexible units (macrocycle, *O*-acetyl group at the 3-position of the lactone and the *O*-isovaleryl group on mycarose and particularly the mycaminose and mycarose sugars). The determination of long-range $^3J_{^{13}C-^1H}$ coupling constants provides important structural information for macrolide antibiotics.[32] This is especially important for the torsion angles of the glycosidic bonds Ψ_1 = H(5)–C(5)–O(5)–C(1′); Ψ_2 = H(1′)–C(1′)–O(5)–C(5); Ψ_3 = H(4′)–C(4′)–O(4′)–C(1″) and Ψ_4 = H(1″)–C(1″)–O(4′)–C(4′) studied by selective excitation of the protons H(5), H(1′), H(4′) and H(1″), respectively.

Initially, it was felt that much of the macrocycle conformational information could be deduced from the ^1H–^1H coupling constant data given in Table 2. Our observed values were compared to those of minimised structures, generated by MD study *versus* the different protocols. The torsion angles of generated structures can be correlated, by using Karplus type-equations,[33,34] to the corresponding calculated coupling constants in Table 3.

An analysis of the $^3J_{H,H}$ values was also used to compare the major solution state conformation of josamycin with that in the crystalline state. The observed vicinal coupling constants confirm that josamycin exists in solution as a major conformation which is very similar to the solid state conformation (Table 3). The fact that the aldehyde group, the lactone CO(1) and the OH at the C(9) position in the lactone ring are all situated above the ring might play an important role in the biological activity of josamycin.

A specific characterisation of a 'folded in' orientation of the H(3) proton in **M1** (Fig. 3a) will be given by the use of the $^3J_{H2pS,H3}$ ($^3J_{H2a,H3}$ = 1.0 Hz) and $^3J_{H4,H5}$ ($^3J_{H4,H5}$ = 9.5 Hz) coupling constants: H(2pS) and H(3) are either *gauche* (+60°) in **M1** or *trans* (170°) in **M2** and **M3**, while H(4) and H(5) are either *trans* (175°) in **M1** or *eclipsed* (+130°) in **M2** and *gauche* (+75°) in **M3**, respectively (Fig. 3a). The experimental coupling

Table 3 Coupling constants (^3J/Hz) calculated from the different conformations generated by MD for josamycin

			J_{calc} [c]				
Vicinal pair	J_{exp} [a]	$J_{X\text{-}ray}$ [b]	**M1**	**M2**	**M3**		
J_{HH} (Macrocycle)							
H(2b′), H(3) (2pR)	11.4	12.0	12.3	1.6	2.6		
H(4), H(5)	9.5	12.1	12.3	6.2	2.3		
H(6), H(7b) (7pR)	12.3	12.1	12.4	12.1	12.3		
H(9), H(10)	9.8	9.8	9.8	9.4	12.4		
J_{CH} (Glycosidic bond)			**D1**	**D2**	**D3**	**D4**	
H(5), C(1′)	4.0	5.2	5.4	4.5	5.2–3.4	5.2	
C(5), H(1′)	1.5	2.0	2.0–3.0	2.5	4.3–5.4	5.3	
			C1	**C2**	**C3**	**C4**	**C5**
H(4′), C(1″)	2.0	6.2	6.8	6.1	5.2–4.3	5.6	2.5
C(4′), H(1″)	1.5	5.0	5.4–4.3	2.0	3.5	5.4	1.0

[a] Vicinal proton–proton coupling constants (^3J/Hz) for josamycin in D_2O buffered solution. [b] $S_{X\text{-}ray}$: **M1D1C1** (**S1**), initial structure built from the X-ray crystal structure of demycarosyl-josamycin. [c] Conformations have been defined according to notation in Table 1.

constants ($^3J_{H2a,H3}$ = 1.0 Hz and $^3J_{H4,H5}$ = 9.5 Hz) are in agreement with a major presence of the low-energy conformation **M1** (Tables 2 and 3). Additionally, the extreme values of the observed coupling constants ($J_{H2pR,H3}$ = 11.4, $J_{H2pS,H3}$ = 1.0, $J_{H3,H4}$ = 1.5, $J_{H5,H6}$ = 1.0, $J_{H6,H7}$ = 12.3, $J_{H13,H14}$ = 11.0 and $J_{H14,H15}$ = 12.5 Hz) and the calculated ones would correspond effectively to the predominant **M1** conformation.

The two conformations of josamycin, **M1** with the H(3) proton 'folded-in' and the 3-*O*-acetyl group in a position 'up' above the macrocycle and **M2** with this group in an '*exo*' orientation (Fig. 3a) might be compared to the two types of conformations found in erythromycin derivatives.[35,36] Comparison of erythromycin and josamycin suggests that their stable preferred conformations are different in the C(3)–C(5) region. Looking at the values of homonuclear ^3J coupling constants for the lactone ring, one can see that the overall conformation of the aglycone is significantly different between josamycin and erythromycin. Two types of conformations, **A** and **B**, have to be considered for roxithromycin and erythromycin, the major change being the inward folding of the C(3) fragment in **B** and the outward folding of C(3) in **A**, respectively. Their observed $^3J_{H,H}$ values in the C(3)–C(5) region correspond to the major **A** conformation with the H(3) proton 'folded-out' and the desosamine sugar essentially perpendicular to the macrocycle (**D1** conformer). The minor **B** conformation with the H(3) proton 'folded-in' and the sugar moiety tilted up,[36] participates a little more in solution, for erythromycin than for roxithromycin. The steric effect of the oxime chain in roxithromycin, and the slight steric effects of the 3-acetyl, 4-OMe, 6-aldehyde and 16-Me groups in josamycin, tend to fix the movement of the aglycone ring.

The major difference between **M1**–**M3** conformations is observed in the C(3)–C(5) region which could be related to a different position or motion of the *O*-acetyl group bonded to C(3) and the steric effect of the bulky OMe(4) group. The motion of the formylmethyl(6) group is not of great consequence. Coupling constants relative to C(6)–C(18) reveal that the formyl group is in a major parallel position ($\varphi_{H6H18pS}$ = 180°) with respect to the macrocycle as it is in the major structures generated from molecular modelling calculations (Fig. 3b). It was therefore observed during simulations that an internal rotation occurred around the C(6)–C(18) bond leading to a minor perpendicular position ($\varphi_{H6H18pS}$ = 70°).

The macrocycle flexibility induced five different orientations, **D1**–**D4**, for the mycaminose sugar. The measurement of heteronuclear long-range $^3J_{^{13}C-^1H}$ coupling constants by selective 2D INEPT[32] combined with studies by MD (Table 3) was useful to identify the positions and mobility of the mycaminose sugar with respect to the aglycone (Fig. 4). This is of particular interest since it can be related to the different biological properties of the macrolides. The glycosidic bond torsion angles Ψ_1 = H(5)-C(5)–O(5)–C(1′) and Ψ_2 = H(1′)–C(1′)–O(5)–C(5) were studied by selective excitation of the protons H(5) and H(1′), respectively. Experimental values (J_{Ψ_1} = 4.0 Hz and J_{Ψ_2} = 1.5 Hz) are discussed with regard to the calculated values in the different **D1**–**D4** conformers for the lowest energy structures (Table 3). The mycaminose sugar adopts a conformation **D1** or **D2** ($\Psi_{H1'C4} \approx 50°$, $J_{\Psi_2} \approx 2.5$ Hz) with an orientation perpendicular to the macrocyclic lactone ring and a conformation **D3** ($\Psi_{H1'C4} \approx -30°$, $J_{\Psi_2} \approx 4.5$ Hz) or **D4** ($\Psi_{H1'C4} \approx 150°$, $J_{\Psi_2} \approx 5.5$ Hz) with the two units in the same plane. The **D4** conformation exhibits a turned-back mycaminose. The presence of the major **D1** conformation should increase the coupling constant corresponding to Ψ_1 and, at the same time, decrease that of Ψ_2. However, the participation of the other conformations should decrease the value of J_{Ψ_1} and increase that of J_{Ψ_2}. The observed values for J_{Ψ_1} (4.0 Hz) and J_{Ψ_2} (2.0 Hz) should include a large participation of conformer **D1**, in equilibrium with the model **D3** and this was confirmed by NOE experiments.

The mycarose sugar adopts either conformation **C1** or **C2** ($\Psi_{H4'C1''} \approx 170°$, $J_{\Psi_3} \approx 6.5$ Hz) with a 'down' perpendicular glycosidic bond or conformations **C3**–**C5** ($-20° \leqslant \Psi_{H4'C1''} \leq +50°$, $J_{\Psi_3} \approx 4.5$–2.5 Hz) with an 'up' perpendicular glycosidic bond (Fig. 5). The observed values for J_{Ψ_3} and J_{Ψ_4} in Table 3 ($\leq$ 2 Hz) should include a large participation of conformer **C5**. The presence of this major conformation should decrease the coupling constants corresponding to Ψ_3 and Ψ_4.

All these conclusions will be further tested using molecular dynamic experiments.

1.1.3 Nuclear Overhauser enhancement (NOE). The volumes of the cross-peaks were integrated and later classified by order of magnitude as large, medium or small NOEs. Typical contacts through space are reported in Table 4.

The similarity between the geometry in solution and several MD conformers was also investigated from comparison between the spatial proximity values computed from the different conformations (Table 5) with the observed NOE values (Table 4). For clarity, only intra- or inter-unit contacts of interest are reported in Table 5. Differences between macrocycle types were observed concerning some NOEs, particularly those from H(11) such as {11}3 expected for model **M1** while {11}4 characterised models **M2** and **M3**. This latter NOE is missing for josamycin. The intra-aglycone NOE {13}3, is only present in the **M1** conformation and is also observed in solution.

For the orientation of the mycaminose unit in josamycin, the sugar–lactone NOEs from H(1′), {1′}OMe(4), H(5) suggest that the position of this unit is relatively restrained or corresponds to a major perpendicular orientation **D1**. When the mycaminose sugar makes a **D1**↔**D2** interconversion, three mycaminose–lactone NOEs are expected, {2′}7pR, {5′}5 and {5′-Me}5 but these NOEs were not observed in buffered solution since there is low participation of **D2** conformation. In the same way, the NOE {3′-N(Me)$_2$}OMe(4) characteristic of **D3**, the connectivities {4′}5 and {5′-Me}OMe(4) indicating an orientation **D4** of the mycaminose unit are missing for josamycin.

Analysis of NOE intensities shows interesting mycarose–mycaminose inter-unit contacts but no mycarose–aglycone contacts. The short distance contacts {1″}3′, 4′, Me(5′) such as {2″}Me(5′), {5″}4′ and {5″-Me}3′-N(Me)$_2$, Me(5′) NOEs appear to indicate restraint in the rearrangement of the mycaminose and mycarose moieties. Both sugar rings are oriented approximately perpendicular to the macrolide ring with the 5′-Me and 5″-Me substituents pointing up. No contacts with the macrocycle confirm the shift of mycarose away from the macrocycle and denote a perpendicular position of the two sugar rings **C3**–**C5**, especially if one observes the connectivity between 3′-N(Me)2 and 5″-Me. Contacts of the mycarose with the aglycone are non-existent in josamycin, showing thus a total release of this unit that was no longer maintained by a bent linking of the two sugars. Concerning the mycarose, no contacts with the *O*-isovaleryl chain are found in the molecule. These observations suggest that the *O*-isovaleryl chain on mycarose presents more degrees of freedom and may fluctuate between relatively close positions.

1.2 Molecular modelling. We performed computational chemical studies (molecular dynamics and molecular mechanics calculations), starting with the X-ray crystal structure of demycarosyl josamycin,[8] with the mycaminose sugar modified to include a sugar ring (mycarose) at the 4′-position and a protonated amino group at the 3′-position. A second minimisation was performed from different initial structures generated in the very first trial (Fig. 7) and a third set of calculations was performed with distance constraints based on the observed NOE and TRNOE data. Finally, minimisation was performed releasing all constraints. Lastly the constraints corresponding to inter-unit NOEs were introduced in the form of a quadratic potential with a 2 Å lower limit and a 5 Å upper limit.

Table 4 Qualitative nuclear Overhauser enhancement data and observed TRNOEs for josamycin in D_2O–DMSO (20:80) and D_2O buffered solutions

	NOEs[a]		TRNOEs[b]	
^{1}H observed	Intra-cycle	Inter-cycle	Intra-cycle	Inter-cycle
2a	—		—	
2b	2a (l)		2a (l)	
3	2a (s); 2b (s)		2a (m); 2b (s)	
4	2a (m); 2b (s); 3 (m)			
4-OMe	4 (m); 3 (s); 2a (l); 2b (s)	1′ (s)	2a (m); 2b (m)	1′ (m)
5	4 (s); 3 (s)	1′ (m)	19 (s)	1′ (l); 5′ (s); 5′-Me (s)
6	5 (m); 4 (s); 3 (m)		5 (s); 3 (m); 19 (s)	
7a	—		6 (m); 3 (s); 4 (s)	
7b	7a (l); 18b (s); 6 (s); 4 (s)		7a (l)	
8	7b (m); 18b (s); 6 (m)		18b (s); 18a (l); 7b (s)	
8-Me	8 (m); 6 (s); 4 (m); 3 (s)		8 (l); 7b (l); 18a (s)	
9	8-Me (s); 8 (m); 18a (m); 6 (m)		8-Me (s); 8 (m); 18a (m); 6 (m)	
10	9 (s); 8-Me (m)		9 (s); 8-Me (m); 7a (s)	
11	10 (s); 9 (m); 6 (s); 3 (s)		9 (m); 10 (s); 6 (s); 3 (s)	
12	11 (s); 10 (s)		11 (s); 10 (m)	
13	12 (s); 11 (s); 3 (s)		12 (s); 11 (m)	
14a	13 (s); 12 (m)		13 (s); 12 (m)	
14b	14a (l); 13 (s); 12 (s)		14a (l); 13 (m); 12 (s); 9 (m)	
15	14a (s); 14b (m); 13 (s)		14a (m); 14b (m); 11 (s); 3 (m)	
16-Me	14a (s); 14b (s); 15 (m)		14a (m); 14b (m); 15 (m)	
17-Me	—		—	
18a	18b (l); 6 (s); 19 (s)		18b (l); 6 (m); 19 (m)	
18b	6 (s); 19 (s)		6 (s); 19 (m)	
19	—		—	5′-Me (m)
20	—		—	
21	20 (s)		20 (m)	
21-Me	—		21 (m); 20 (s)	
1′	—		—	
2′	1′ (s)			
3′	2′ (l); 1′ (l)	1″ (s)	1′ (s)	
3′-$N(Me)_2$	—	5″-Me (s)	3′ (s)	1″ (m); 5″ (m); 5″-Me (m)
4′	3′ (m); 2′ (s)	5″ (s); 1″ (s)		1″ (l)
5′	4′ (m); 3′ (m); 1′ (m)		1′ (l); 3′ (l); 4′ (m)	1″ (m)
5′-Me	5′ (s); 4′ (s)	2″-*ax* (s); 1″ (m); 5″-Me (s)	5′ (m); 4′ (s)	2″ (m); 1″ (l)
1″	—		—	
2″-*eq*	—			
2″-*ax*	1″ (l)		1″ (l)	
3″-Me	2″-*ax* (l)		1″ (s); 2″ (l)	
4″	3″-Me (s); 2″-*ax* (s); 2″-*eq* (s); 1″ (s)		3″-Me (s); 2″ (s)	
5″	—		—	
5″-Me	5″ (s); 4″ (s)		5″ (m)	

[a] Observed ^{1}H NOE data from 2D ^{1}H NOESY (τ_m = 800 ms, NOEs > 0). [b] TRNOESY (ribosomes 2 μM, τ_m = 150 ms, TRNOEs < 0) experiments in D_2O buffered solution (≈2 mM) at 293 K and pH = 7.6. 2D ^{1}H NOESY map, τ_m = 150 ms, in D_2O buffered solution (≈2 mM) pH = 7.6, is empty.

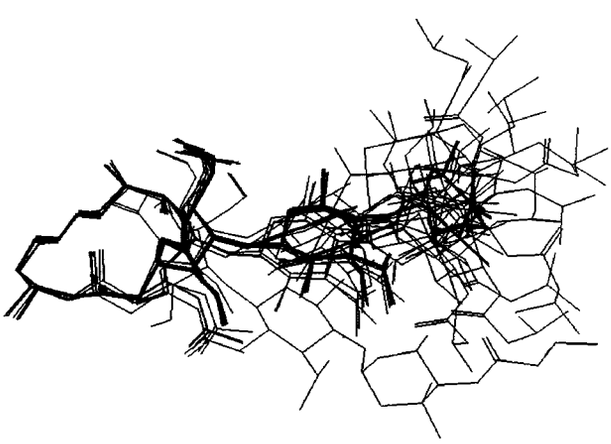

Fig. 7 Superimposition of the 17 lowest energy conformations (**S1**–**S17**) generated in the very first trial after preliminary conformational explorations with periodic temperature jumps to 600 K.

The final structures obtained after several such calculations were examined for their overall energetic favourability and compared with the structure derived from the NMR data. The aims of this work are to use MD calculations, (i) to determine the flexibility of the sugar rings about the glycosidic bonds and predict the available conformational space for the mycaminose, and (ii) to determine the rotational freedom about the endocyclic dihedral angles in the macrocycle and thus, on the basis of the minimum energy level, to generate the approximate ratios of minimum-energy conformations available up to 1–3 kcal mol^{-1}. Structures found to have a higher energy, up to 10 kcal mol^{-1}, are representative of very hindered intermediates. The 17 lowest energy conformations resulting from this study are listed in Table 6 and these conformers will be referred to from here on by the names in this Table. The global minimum was found in the very first trial (Fig. 7), and the lowest energy conformations (Fig. 8) were found to be **S3** and **S5** (≈83 kcal mol^{-1}).

Table 6 summarises the exploration of conformational space covered during MD simulations, potential energy and the main values of some homo- and heteronuclear dihedral angles of minimised structures. Values of coupling constants (Table 3) are estimated by Karplus type equations [33,34] and are compared to the observed vicinal coupling constants to estimate conformational equilibrium. The similarity between the geometry in solution and several MD conformers was also investigated from comparison between the spatial proximity values computed from the low-energy conformers (Table 5) with the observed NOE values.

Table 5 Inter-proton distances (2–4 Å) from minimised structures derived from MD

Connectivities[a]	**M1**	**M2**	**M3**	NOEs	TRNOEs		
Intra-macrocycle							
4–2pR	m	m	m	s	m		
4–2pS	l	l	m	m	l		
4OMe–2pR	l	s	m	s	l		
4OMe–2pS	l	m	l	l			
5–3	m	l	l	s			
6–3	l	l	m	m	l		
7pS–4	l	l	l	s			
7pS–6	l	l	l	s			
8Me–4	s	s	a	m			
8Me–7pS	l	l	l		l		
10–3	m	a	a				
10–7pS	l	l	m		m		
11–3	m	s	a	s	m		
11–4	a	m	m				
11–4OMe	a	a	m				
11–6	m	m	l	s	m		
12–3	m	a	a				
13–3	s	a	a	s			
15–3	s	a	a		m		
16Me–14pS	l	l	l	s			
16Me–14pR	m	l	l	s			
18pR–9	l	m	l	m	l		
19–9	a	a	m				
Macrocycle–mycaminose	**D1**	**D2**	**D3**	**D4**	NOEs	TRNOEs	
1′–4OMe	m	m	s	m	s	m	
1′–5	l	l	l	m	m	l	
2′–7pR	m	m	s	s			
2′–17Me	a	a	a	m			
2′–19	a	a	a	m			
3′–17Me	a	m	a	a			
3′$N(Me)_2$–4OMe	a	a	m	a			
3′$N(Me)_2$–18pS	a	a	a	m			
4′–5	a	a	a	m			
4′–17Me	a	a	a	m			
5′–5	m	m	s	s		s	
5′–18pS	s	a	m	a			
5′Me–4OMe	a	a	a	m			
5′Me–5	m	m	a	s		s	
5′Me–19	m	s	a	a		m	
1″–17Me	a	m	a	s			
5″Me–17Me	a	a	a	m			
Mycaminose–mycarose	**C1**	**C2**	**C3**	**C4**	**C5**	NOEs	TRNOEs
1″–1′	m	s	a	a	a		
1″–2′	s	s	a	s	a		
1″–3′	l	l	s	s	s	s	
1″–3′$N(Me)_2$	m	l	m	l	a		s
1″–4′	m	m	l	l	m	s	l
1″–5′	l	m	m	s	m		s
1″–5′Me	m	s	l	m	l	m	m
3″Me–3′$N(Me)_2$	s	a	a	a	a		
3″Me–5′Me	a	a	a	m	a		
5″–3′$N(Me)_2$	a	a	l	l	l		l
5″–4′	m	s	m	s	l	s	
5″–5′	s	l	a	s	a		
5″–5′Me	l	l	a	s	m		
5″Me–3′$N(Me)_2$	a	a	l	l	m	s	s
5″Me–5′	s	l	a	a	a		
5″Me–5′Me	l	s	a	a	m	s	

[a] Some evident contacts intra-unit found for the different structures are not specified: a, absent; s, small; m, medium; l, large.

1.2.1 Molecular dynamics. The molecular dynamics (MD) simulations were carried out using the force field, CVFF (as implemented in BIOSYM).[37]

1.2.1.1 Protocol I For a preliminary conformational exploration, after energy minimisation and an equilibration period, we performed a 50 ps MD run at 300 K with periodic temperature jumps to 600 K to supply the system with energy (to pass conformational barriers). The simulation was stopped every picosecond, and the remaining structure energy minimised. When the MD sampling efficiency is low, the method of multiple starting points may help to improve the result (Table 7).[38] Starting from different conformations (five, here) in order to better sample phase space seems more efficient than a very long MD run.[38] Molecules of lowest energies generated during this experiment are mainly of **M1D1C1** (40%) and **M1D1C3** (32%) types with a substantial participation of **M1D3C3** (16%) (Fig. 9a). The minor conformations **M2** and **M3** correspond to structures of "higher energy" (13.4 and 6.3 kcal above the minimum, respectively).

All the conformers resulting from this experiment exhibit

Table 6 Energies and torsion angles (in degrees) computed for the structure families of josamycin represented by 17 low energy conformations

Family	Structures	Conformation	H(4)–H(5)	H(2pR), H(3)	Ψ_1	Ψ_2	Ψ_3	Ψ_4	E_p/kcal mol^{-1}
S_I			175	175	10–15	45–55			
	S1	**M1D1C1**					170	10–25	87.6
	S2	**M1D1C2**					−160	55	88.8
	S3	**M1D1C3**					15–25	40	83.3
	S4	**M1D1C4**					−20	−10	84.9
	S5	**M1D1C5**					35–55	85	83.2
S_{II}			175	175	−15	−25			
	S6	**M1D3C1**					170	10–25	88.0
	S7	**M1D3C2**					−160	55	89.4
	S8	**M1D3C3**					15–25	40	84.0
	S9	**M1D3C4**					−20	−10	84.9
	S10	**M1D3C5**					35–55	85	88.8
S_{III}			175	175	15	150			
	S11	**M1D4C4**					15–25	40	85.6
	S12	**M1D4C4**					35–55	85	91.5
S_{IV}			130	−85	25	50			
	S13	**M2D2C1**					170	10–25	96.6
S_V			−70	−70	10–15	48–55			
	S14	**M3D1C1**					170	10–25	93.4
	S15	**M3D1C3**					13–26	40	89.5
	S16	**M3D1C4**					35–55	85	92.0
S_{VI}			−70	−70	−40	−10			
	S17	**M3D3C1**					170	10–25	96.4

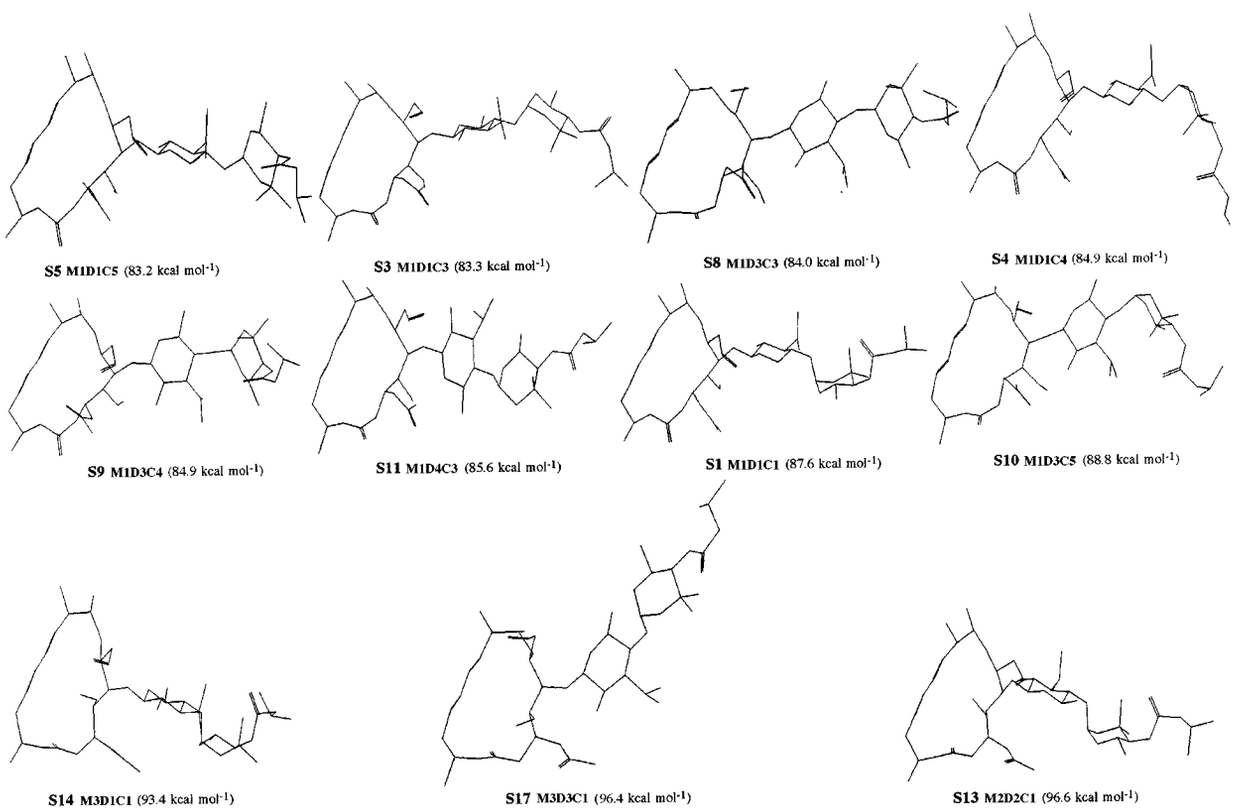

Fig. 8 View of some different structures generated by a systematic conformational search for josamycin: **S5** (**M1D1C5**) $E = 83.2$ kcal mol^{-1}; **S3** (**M1D1C3**) $E = 83.3$ kcal mol^{-1}; **S8** (**M1D3C3**) $E = 84.0$ kcal mol^{-1}; **S4** (**M1D1C4**) $E = 84.9$ kcal mol^{-1}; **S9** (**M1D3C4**) $E = 84.9$ kcal mol^{-1}; **S11** (**M1D4C3**) $E = 85.6$ kcal mol^{-1}; **S1** (**M1D1C1**) $E = 87.6$ kcal mol^{-1}; **S10** (**M1D3C5**) $E = 88.8$ kcal mol^{-1}; **S14** (**M3D1C1**) $E = 93.4$ kcal mol^{-1}; **S17** (**M3D3C1**) $E = 96.4$ kcal mol^{-1}; **S13** (**M2D2C1**) $E = 96.6$ kcal mol^{-1}.

both **M1** (98%) and **M2** or **M3** (2%) conformations with populations **D1** (78%), **D2**, **D4** (1%) and **D3** (20%) of the mycaminose sugar while the mycarose ring presented **C1** (44%), **C2** (5%), **C3** (48%) and **C4** (3%) types. The observed structure confirmed the tendency of the mycarose **C1** and **C3** types to move away from the mycaminose sugar which adopts a perpendicular **D1** or a planar **D3** orientation with respect to the macrocycle when the *O*-isovaleryl chain is not directed towards the mycarose. The structure from MD with the sugar ring **C3** is more stable by 4.3 kcal than the other, **C1** (Fig. 8). Molecules of lowest energies generated during this experiment are mainly of the **M1** conformation, involving both **D1** and **D3** conformations in the same range of energy. In this protocol, the **D3** conformer is stabilised by hydrogen bonding involving OMe(4), [2′-OH · · · OMe(4)] while [2′-OH · · · O(5)] stabilises the conformer **D1**.

This detailed analysis indicated that josamycin exists in equilibrium with different conformations. Thus, after finding conformations, one needs to produce an effective ensemble in which all of the most significant conformers have been located (Fig. 9a). Other minor conformations participate a little in solution. The stability of the different conformers has been

Table 7 Simulations using temperature jumps at 600 K with relative permittivity $\varepsilon = 4\ r$ starting from $\mathbf{S}_{\text{X-ray}}$ structure and some arbitrary conformations representing various families[a]

		Starting **S** conformations (frequency)																
Family	**S**	Conformation	$\mathbf{S}_{\text{X-ray}}$[b]	**S1**[b]	**S8**[b]	**S14**[b]	**S17**[b]	Total frequency (≥5%)		$\mathbf{S}_{\text{X-ray}}$[c]	**S3**[c]	**S5**[c]	**S11**[c]	Total frequency (≥5%)		$\mathbf{S}_{\text{X-ray}}$[d]	**S3**[d]	**S5**[d]	Total frequency (≥5%)	
$\mathbf{S_I}$	**S1**	**M1D1C1**	x (34)	x (31)		x (34)		99	40%											
	S2	**M1D1C2**	x (4)	x (5)				9		x (11)				11	6%					
	S3	**M1D1C3**		x (6)	x (33)	x (14)	x (26)	79	32%					—		x (31)	x (31)	x (23)	85	57%
	S4	**M1D1C4**			x (2)	x (2)	x (3)	7		x (33)	x (3)			36	18%	x (3)	x (11)	x (1)	15	10%
	S5	**M1D1C5**					x (1)	1		x (3)	x (36)	x (43)	x (46)	128	64%					
$\mathbf{S_{II}}$	**S6**	**M1D3C1**	x (3)					3						—						
	S7	**M1D3C2**	x (4)					4						—						
	S8	**M1D3C3**		x (8)	x (14)		x (17)	39	16%					—		x (8)	x (3)	x (13)	24	16%
	S9	**M1D3C4**					x (2)	2		x (3)				3		x (5)	x (5)	x (4)	14	10%
	S10	**M1D3C5**						—			x (11)	x (7)	x (4)	22	11%					
$\mathbf{S_{III}}$	**S11**	**M1D4C3**			x (1)			1												
	S12	**M1D4C4**						—								x (3)			3	
$\mathbf{S_{IV}}$	**S13**	**M2D2C1**	x (2)					2												
$\mathbf{S_V}$	**S14**	**M3D1C1**	x (1)					1												
	S15	**M3D1C3**					x (1)	1										x (8)	8	5%
	S16	**M3D1C4**						—										x (1)	1	
$\mathbf{S_{VI}}$	**S17**	**M3D3C1**	x (2)					2												

[a] Each column represents one simulation, a 50 ps MD run at 300 K with periodic temperature jumps to 600 K and 'x' indicates that the conformation was found. The frequency is the number of times each conformation was found. Calculations were performed [b] for a preliminary conformational exploration, then with distances constraints based on the observed [c] NOE and [d] TRNOE data. Final minimisation was performed releasing all constraints. Finally the constraints corresponding to NOEs inter-units were introduced in the form of a quadratic potential at 2 Å lower limit and 5 Å upper limit.

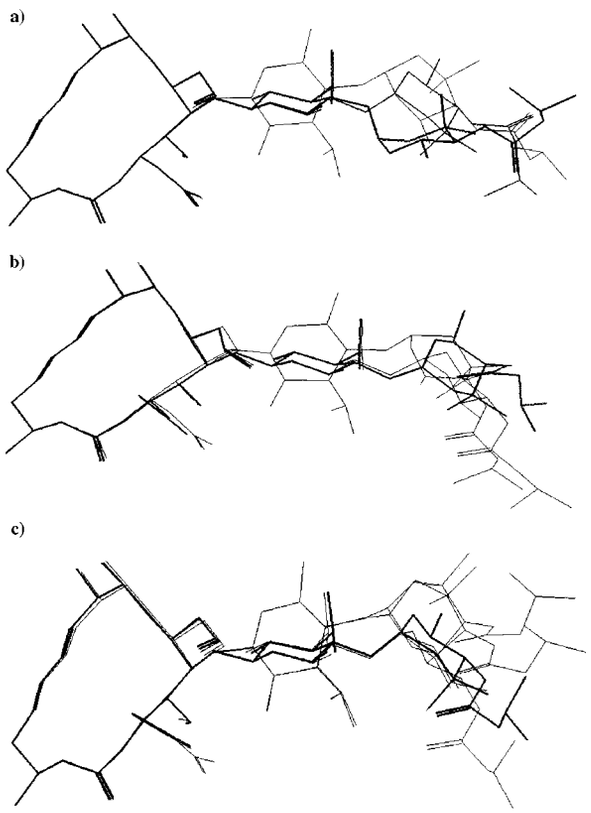

Fig. 9 a) Superimposition of **S1** (**M1D1C1**), **S3** (**M1D1C3**) and **S8** (**M1D3C3**) conformations generated by MD from a preliminary conformational exploration; b) Superimposition of **S5** (**M1D1C5**), **S4** (**M1D1C4**) and **S10** (**M1D3C5**) conformations generated by MD with distance constraints based on the observed NOE data; c) Superimposition of **S3** (**M1D1C3**) and **S8** (**M1D3C3**) conformations generated by MD with distance constraints based on the observed TRNOE data.

tested by a protocol without raising the temperature (300 K) and using a 200 ps timescale with energy minimisation every picosecond. The conformations **M2** or **M3** are not induced with this protocol. The mycaminose sugar was found to be essentially perpendicular to the macrocycle (**D1** conformer). The freeing of the *O*-isovaleryl chain on mycarose allows the mobility around the glycosidic bonds, which is sufficient to induce the coplanar conformation **D3**. Surprisingly, whatever starting structures we used, the **M1D1C3** (55%) and **M1D3C3** (39%) conformations are mainly generated with a little participation of **M1D1C4** (5%) and **M1D3C4** (1%), 1.6 kcal above the minima. The minimum potential-energy structures, **M1D1C3** and **M1D3C3**, are stable during the whole protocol.

1.2.1.2 Protocol II MD simulations were performed from different initial structures with distance constraints based on the observed NOE data. The similarity between an averaged geometry in solution and several MD conformers was investigated from the intensive NOESY correlations observed.

During the MD simulation, the minor structures **M1D1C2** (6%), **M1D3C5** (11%) and **M1D1C4** (18%) underwent conformational averaging (Fig. 9b) with a major participation of the more stable conformer **M1D1C5** (64%).

A comparison between experimental (NMR) and calculated coupling constant values obtained in MD simulations has been made to estimate eventual conformational equilibrium of josamycin in solution. For each conformation obtained from this protocol, coupling constants $^3J_{H,H}$ and $^3J_{C,H}$ have been calculated and compared to the observed vicinal coupling constants (Table 3). The spatial proximity values computed from the low-energy structures in different conformations were also compared with the observed NOE values (Table 5). The predominant **M1D1C5** conformation determined from the theoretical MD structures is in agreement with the experimental NMR results in solution. It is concluded that josamycin exists in solution as one major conformer very similar to the stable conformer **M1D1C5** (Fig. 8).

2. Structural characteristics of josamycin bound to the bacterial ribosome

Taking advantage of the exchange between bound and free macrolide antibiotic, we have developed a study of josamycin–ribosome interactions to *E. coli* ribosomes, using two-dimensional transferred nuclear Overhauser effect spectroscopy (TRNOESY).[10,14–16] The information present in TRNOE analysis focuses on a plausible conformation essential for the substrate's antibacterial action when binding to the bacterial ribosome.

Room temperature seems better for fast exchange upon complex formation and leads to optimal conditions for TRNOESY experiment. The experiments were performed with josamycin in phosphate buffers at apparent physiological pH 7.6. The antibiotic samples were dissolved in an aqueous NaD_2PO_4–Na_2DPO_4 buffer (0.05 M) with KCl (0.2 M). Physical parameters of crucial importance for chemical exchange such as temperature, substrate–ligand ratio and *E. coli* ribosomal concentration have to be optimised.[10] Another parameter has to be refined, the TRNOEs time dependence of 16-membered macrolides (τ_m = 150 ms) to avoid spin diffusion. Likewise, spin diffusion effects appeared for mixing times larger than 150 ms for 14-membered macrolides.

2.1 Josamycin/ribosome ratio. The line-broadening of josamycin is proportional to the amount of ribosome. With 0.8 μM concentration of ribosomes, as for the 14-membered macrolides, the line-broadening was too weak to be detected. High ribosomal concentration (2 μM) with 1 mM fraction of ligand causes half line-broadening of the josamycin signals as well as clearly observable TRNOE cross-peaks. Assuming that the correlation time of the inter-proton vector motion (τ_c) increases in proportion to the molecular mass of the complex, the TRNOEs would be observable even for a large excess of ligand (*e.g.*, 5000 : 1 ratio for 14-membered macrolides).[39] Here, with a 500 ligand/ribosome ratio (like for spiramycin),[40] transferred NOE effects from josamycin–ribosome interactions can be observed only with such concentrations. These results suggested that 16-membered macrolides exhibit a lower affinity for weak ribosomal interaction than the 14-membered macrolides previously studied.[9,10,41]

2.2 Bound conformation. The bound structure of josamycin is blocked into a specific and favoured conformation in weak interaction with *E. coli* ribosomes. In particular, NOEs relative to the **M1D1C3** conformation appear strongly with ribosomes.

2.2.1 The intra-macrocycle TRNOEs. The structures representing the bound state of josamycin show great similarity with the free macrolide ring (**M1** conformation) with NOE interactions between protons {11}3. The new intra-aglycone NOE {15}3 characteristic of the **M1** conformation, is only present in the bound state. Conversely one NOE {4}8Me found in the **M2** conformation, is missing. A comparison of the free and bound **M1D1C3** structure shows the inward folding of the 3-acetyl fragment (Fig. 10b).

2.2.2 The inter-macrocycle–mycaminose TRNOEs. The mycaminose–lactone NOE {5}1′ is observed for free as well as bound structures. This result, showing the spatial proximity of H(1′) to H(5), is exactly that expected if the mycaminose sugar ring is oriented approximately perpendicular to the macrocycle lactone ring, conformation **D1**.

2.2.3 The inter-sugars mycaminose–mycarose TRNOEs. The TRNOEs {1″}5′Me, {1″}4′ and {5″Me}3′-N(Me)$_2$ are observed for the three sugar rings in the bound structure that correspond

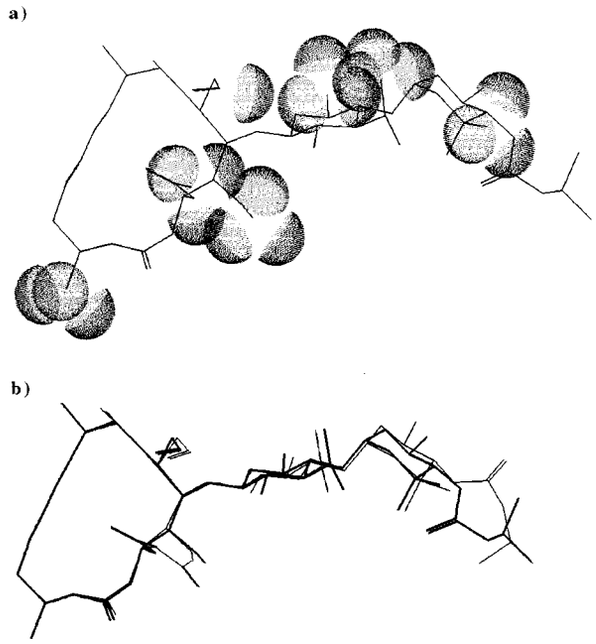

Fig. 10 a) Minimised structure **M1D1C3** from transferred NOEs data (bound to ribosomes) of josamycin. The van der Waals surfaces are shown to indicate the atoms whose signals are most broadened [16-Me, 17-Me, 4-OMe, 5′-Me, 5″-Me, 3″-Me, H(19) and H(21)]. The broadening observed may reflect proximity to a binding surface. b) Superimposition of TRNOESY derived structure in bold, weakly bound to bacterial ribosomes **M1D1C3** $E = 81.9$ kcal mol^{-1} (protocol III) and free conformation **S3** (**M1D1C3**) $E = 83.3$ kcal mol^{-1} generated by MD (protocol I). Quality of superimposition of all the atoms was evaluated by root mean square (rms) deviation between the atoms constituting the bound conformer in bold and the corresponding atoms in the free conformation (rms, 0.3928 Å).

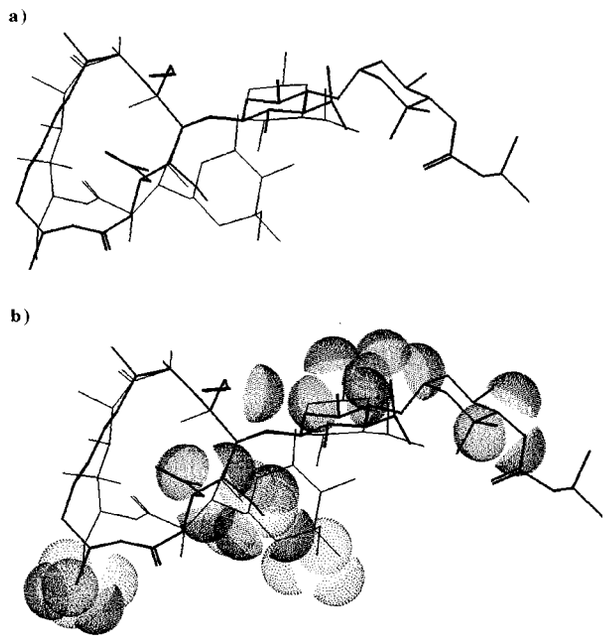

Fig. 11 a) Superimposition of josamycin (in bold) and erythromycin TRNOESY derived structures, weakly bound to bacterial ribosomes. b) The van der Waals surfaces of signals which are most broadened are shown for josamycin (in bold) and erythromycin.

to the same interaction in the free and bound molecules. Three new inter-sugar ring TRNOEs, {1″}3′-N(Me)$_2$, {1″}5′ and {5″}3′-N(Me)$_2$, were present in bound josamycin and were not observed in the corresponding free structure. The spatial proximities of H(1″) and H(5″) to 3′-N(Me)$_2$ are exactly those expected if the mycarose ring is oriented approximately perpendicular to the mycaminose ring, conformation **C3** (**C4**) with Me(5″) pointing up. The main difference between the bound structure **M1D1C3** and the major structure in solution **M1D1C5** is the new NOE {1″}3′-N(Me)$_2$ characteristic of the **C3** conformation and missing in the **C5** one.

2.2.4 Protocol III. Molecular modelling was carried out and TRNOESY data were applied to josamycin. 3 ± 1 Å constraints (upper bound distance 4 Å, lower bound distance 2 Å) were used. All calculations were performed for solvent conditions using in the description of the coulombic interaction in the CVFF Forcefield a distance-dependent relative permittivity fixed to $4 \times R_{ij}$. When TRNOESY data were applied to the structures of the drug and minimised, josamycin gave rise to the low energy structures (Table 7) **M1D1C3** (57%), **M1D1C4** (10%), **M1D3C3** (16%) and **M1D3C4** (10%) shown in Fig. 9c.

From these experiments, the **M1D1C3** conformation appears to be the plausible bound structure relative to this weak specific binding to the bacterial ribosome (Fig. 10a). Indeed, the structure representing the bound state of the drug shows conformational homology with the free **M1D1C3** conformation after superimposition (Fig. 10b). Only the positions of the 3-acetyl group and the *O*-isovaleryl chain show some variation relative to the free state. The conformation of the 16-lactone ring is characterised by the 'up' position of the carbonyl group (1-CO) while the inward folding of the 3-acetyl group leads to an *endo* orientation of its CO group. The positions of the two carbonyl groups (from 3-acetyl and 6-formyl) are maintained by stacking. That may be of importance for the josamycin mode of action as the deacetylated josamycin, a degradation product found after hydrolytic removal of the 3-acetyl, showed no antibacterial activity.[42] On the other hand, it may be considered that the aldehyde group is an important group for antibacterial activity, as the activity of josamycin was markedly decreased when the 6-formyl group in the lactone was modified to the alcohol.[23]

2.3 Binding surface. In general, a correlation between line broadening and involvement in binding is expected. Line broadening in NMR spectra may result from two distinct processes, equilibrium between states with different chemical shifts, and slowing of molecular motion. Macrolides bind to ribosomes at an identical 'surface' of the drug molecule to erythromycin A, involving the C(13)–C(5) lactone region of the aglycone and both sugar rings.

Finally, a model of josamycin showing the hydrogen atom giving the most extensively broadened resonances is constructed (Fig. 10a) using van der Waals' surfaces. The model is based on the minimised structure derived from MD experiments and will be compared to the ones suggested for erythromycin and for roxithromycin (Fig. 11).[9,10,41] The 'surface' of josamycin deduced from the variation in line broadening would be indicative of the relatively rigid part of the molecule. However it is not initially exact for the free molecules. The data corresponding to the C(4)–C(5) region are indicative of near-rigid rotation of these atoms in close proximity to the ribosome due either to a sterically hindered rotation or to specific inter-unit (ribosome–josamycin) bonds involving this region, while conformational instability appears in the C(3)–C(5) region of the free antibiotics in the molecular modelling study. In the free ligand, this portion of the macrocyclic ring can fold outwards so that the 3-*O*-acetyl group in an '*exo*' orientation (Fig. 3) leads to the **M2** conformation.

From these experiments, the **M1D1C3** conformation appears to be the plausible bound structure relative to this weak specific binding to the bacterial ribosome and the broadening observed in the C(16-Me)–O(16)–C(17-Me)–C(4-OMe) region, C(19), C(21), C (5′-Me), C (3″-Me) and C (5″-Me) may reflect proximity to a binding surface. These methyl substituents favour hydrophobic interactions between josamycin and the ribosome at the peptidyl transferase centre.

The structures representing the bound state of the drugs

(josamycin and erythromycin) show conformational homology after superimposition (Fig. 11): the C(4)–C(9) region is almost completely superimposable while variation appears in the 'down' side of the molecule. Because of the presence of the 16-membered macrocycle, the flexible right hand side of the macrolide ring C(2)–C(4) of the major conformation **M1** [H(4)–C(4)–C(5)–H(5), *trans*] exhibits some deviation from the 'folded-out' conformation **A1** [H(4)–C(4)–C(5)–H(5), *eclipsed*] found in erythromycin derivatives. This corresponds to an important variation between 14- and 16-membered macrolide classes as for both, the aminosugar was found to be essentially perpendicular to the macrocycle (**D1** conformer). Thus, the position of the 5-mycaminose sugar is similar in the 16-membered macrolide to that of the 5-aminosugar in other drugs. Superimposition of the bound structures revealed one change that may be of importance for the 16-membered macrolide mode of action, namely a stretching out of the mycarose sugar unit as it is now the terminal unit of a 5-disaccharide. This sugar moiety in josamycin has moved by *ca*. 5 Å away from the C(15) region compared to 5-desosamine in erythromycin where it is directly attached to the aglycone (Fig. 10).

A significant line broadening affected the 16-methyl, the 4-*O*-methyl and the *O*-acetyl group at the 3-position, positioned in the external part of the molecule, close to the 1-CO region. The broadening also involved the 6-CHO group, the functional group important for the appearance of activity in the 16-membered ring macrolides. The broadening observed may reflect proximity of the formyl group to a binding surface involving an additional interaction of the 16-membered macrolide with ribosome. A significant line broadening of the 5′- and 5″-methyl in mycaminose and mycarose units may indicate a proximity of these residues in the 16-membered macrolide–ribosome complex as the line broadening affects the sugar units in other drugs. This may be due to the fact that both 5-disaccharide in josamycin and 5-desosamine in erythromycin bind to the bacterial ribosome, but at different locations, or in a different way. This study can explain some of the significant differences between josamycin and the other antibiotics.

3. Drug–ribosome interactions

The weakly bound state of the josamycin observed here probably represents a first stage in a binding process. The weak interactions observed by NMR are in agreement with a hypothesis of two distinct binding levels, as was reported for ribosome–tetracycline interactions,[43] with a low affinity binding level and the tight inhibition binding one. This weak binding observed by TRNOE experiments could be involved in the first step of recognition and selection of macrolide antibiotics by the ribosomal machinery.

Compounds which are not able to take part in a weak binding interaction with bacterial ribosomes do not exert antibiotic activity,[10] as also observed by Barber *et al.*[14,44] Thus, the weak binding site seems to be a necessary step for the strong interaction.

To distinguish here between the specific effects of drugs binding to their targets and non-specific interactions between small molecules and macromolecular complexes, ribosomal 'core' particles were prepared by incubating 50S subunits with 1.3 M LiCl solution to remove the outer proteins.[45] Cores were used in place of whole ribosomes with josamycin in control experiments. Spectra were run of josamycin alone, in the presence of 2 μM ribosomes (a concentration determined to give a significant increase in line width) and separately in the presence of 4 μM cores. The concentration of josamycin was 1 mM and the buffer solution in each case was potassium phosphate buffer 50 mM with KCl 200 mM. The addition of ribosomal cores to josamycin resulted only in a slight broadening of all the lines in the control spectrum and a blank TRNOESY spectrum. This indicates that the only interactions between josamycin and ribosomal core particles are non-specific. It was clear from these data that the active 16-membered macrolide bound weakly to bacterial ribosomes in a similar way to the erythromycin A group, as indicated by selective line broadening in the ^{1}H NMR spectra.

The macrolides have similar chemical characteristics but display dissimilar inhibitory properties. The 16-membered macrolides are considered to be typical inhibitors of peptide bond formation while the erythromycin group (14-atom lactone ring) is an inhibitor of peptidyl-tRNA translocation. The difference in the mode of action of the two macrolide groups can be attributed to the different glycosidic substituents and not to the size of the lactone ring. The different macrolide groups seem to compete for binding to the ribosomes, indicating the existence of overlapping sites of interaction.[46] Members of the erythromycin family apparently block protein synthesis only after the formation of several peptide bonds due to steric hindrance by the drug molecule.[47,48] The 16-membered macrolide exerts its effects in the very early stage of peptide bond formation.[17] The drug-binding site is probably displaced some distance along the exit route of the nascent peptide chain, and only the 16-atom ring macrolides carrying larger disaccharide substituents, are able to interfere with peptide bond formation.[49] We have investigated the effect of the addition of a 0.13 mM amount of josamycin to an erythromycin–ribosomal solution and the resonance lines of erythromycin narrow with increasing josamycin concentration. On reversing the experiment (addition of erythromycin to a josamycin–ribosome solution until a 1:1 ratio of macrolides is reached), the opposite situation prevails, and the resonance lines of josamycin widen with increasing erythromycin concentration. The results obtained in these assays seem to confirm that the two groups of macrolides also have overlapping weak binding-sites.

Conclusion

It was shown that the effect of the macrolide class was similar for josamycin compared to erythromycin and roxithromycin. The overall conformation of the macrolactone ring was not changed to a significant degree. The NMR data indicate that although more than one conformer is present in solution, one conformer dominates (**M1D1C5**). The set of proton–proton coupling constants and nuclear Overhauser effects as well as molecular modelling data yield a structure for the predominant conformer. A combination of NMR spectroscopy and molecular modelling techniques showed that the major solution state conformation is a 1-CO 'up' type, while the contribution of the '*endo*' and '*exo*' 3-acetyl group, 6-formyl and *O*-isovaleryl chain (on mycarose) conformers in the solution is observed.

In the bound structures (**M1D1C3**) (Fig. 10a), the data indicated that the two 3-acetyl and 6-formyl groups are anchored to the aglycone above the 16-membered ring and their two carbonyls are maintained inward by stacking. The positions of the two sugar rings are different in the major solution and bound structures. The orientation of the mycarose and the chain are opposite, 'up' and 'down', respectively (Fig. 10). In the ribosome complex, as evidenced from the constraints of the different TRNOEs observed in D_2O solvent, the active molecules require similar orientation of one sugar (conformation **D1** perpendicular to the macrocycle) compared to 14-macrolides, while the second sugar ring, the 4-methoxy group and the C(13)–C(15) region may vary. The mycarose sugar moiety in josamycin has moved by *ca*. 5 Å away from the C(15) region compared to erythromycin.

Here also, TRNOEs NMR experiments were proved to be efficient for the location and detection of the weak interactions due to ribosomal activity providing a relationship between conformation in interaction and activity. Shifting of the sugar rings, modification of the C(4)–C(5) bond angle, absence of steric hindrance in the 3-C area and additional implication of

the 6-formyl group in the binding surface maintained inward by stacking with the 3-acetyl group, all these properties may be of importance for the 16-membered macrolides' mode of action. These results can explain some of the differences observed between josamycin and 14-membered macrolides (lower ratio, similar temperature dependence and spin diffusion effect). Thus, josamycin exhibits a lower affinity for weak ribosomal interaction than other macrolides.

Experimental

NMR

The sample was dissolved in an aqueous NaD_2PO_4–Na_2DPO_4 buffer (0.05 M), with KCl (0.2 M) at physiological apparent pH 7.6 and it was possible to attain concentrations of 1.5 mM for ^{1}H experiments. To improve its solubility in aqueous solution we had to first dissolve josamycin in a minute amount of DMSO-d_6, and thus, we could attain concentrations of 4 mM. A crystal of $TSPD_4$, 3-(trimethylsilyl)[2,2,3,3-d_4]propionic acid, sodium salt, was used as internal reference for the proton shifts. The errors on the chemical shifts are 0.01 ppm for ^{1}H.

The experiments were run at 500 MHz for ^{1}H, at 293 K, on Bruker AMX 500 Spectrometers equipped with a Silicon Graphics workstation. A presaturation of the solvent was used for all the 1D and 2D ^{1}H experiments.

Measurement of long-range heteronuclear (^{13}C–^{1}H) coupling constants. Three bond ^{13}C–^{1}H coupling constants were measured using a selective 2D INEPT[32] experiment. At 500 MHz, selectivity was achieved by a 180° DANTE type pulse train *via* the decoupler channel. 64 Experiments were carried out then data were zero-filled to 256 points in the F_1 dimension. In the F_2 dimension, data were acquired with 2048 points and no zero-filling was applied. Resolution enhancement by Gaussian transformation was realised in the F_1 dimension. The D_0 delay was initially set to a value of 3 μs and was increased by 17 ms between experiments.

NOESY experiments. The 2D phase-sensitive ^{1}H NOESY experiments were performed using the States-TPPI method and volume integration of cross-peaks was made with the PARIS algorithm of the GIFA software. FIDs were acquired over 5555 Hz into a 2K data block for 512 increment values of the evolution time, t_1. The raw data were zero filled to a 2K × 2K matrix. Experiments were performed with different mixing times of 400, 600 and 1000 ms and the relaxation delay D_1 was 1.5 s.

^{1}H TRNOESY experiments. The applications in TRNOESY include ligand/receptor ratios usually less than 50. Here with a large value of the k_{off}, transferred NOEs effects from macrolide–ribosome interactions could be observed with a 500 ligand/ribosome ratio. Microdialysis on MF-type Millipore membrane filters with 0.025 μm pore size was done in advance to remove TRIS impurities present during ribosome isolation. Concentration of 2 μM of *E. coli* MRE 600 strain 70S ribosomes is appropriate because it gives a significant increase of the line width of josamycin.

The 2D phase-sensitive ^{1}H TRNOESY experiments in D_2O buffered solution were performed by the States-TPPI method using a mixing time of 150 ms. FIDs were acquired (64 scans) over 5555 Hz into a 2K data block for 256 incremental values of the evolution time and a relaxation delay of 2 s. Water suppression was performed by a low power transmitter pulse of presaturation (60 dB) during relaxation delay and mixing time. One half-sinusoid (5% truncated) shape homospoil gradient of 10 G cm^{-1} was used during mixing time.

Molecular modelling

The calculations were run on a Silicon-Graphics computer using the CVFF Forcefield from Dauber-Osguthorpe and Hagler[37] of Biosym software 'INSIGHT II' and 'DISCOVER'.

Josamycin structure was built from the crystallographic coordinates of the solid demycarosyl–josamycin as a starting point and atomic potentials and charges were recalculated using the built-in algorithm of the program.[50] For the electrostatic energies, since no explicit solvent molecules were incorporated during the run, the relative permittivity was set distance-dependent ($\varepsilon = 4\ R_{ij}$), in order to mimic the solvent effect. For the Molecular Dynamics calculations, the trajectories were calculated by means of the Verlet Algorithm used in the force-field of DISCOVER. The starting structures were first minimised using 100 steps of the 'Steepest Descent' algorithm and then the 'Conjugate Gradients' algorithm until a convergence of 0.1 kcal mol^{-1} was reached. The system was then equilibrated over a period of 6 ps to reach a temperature of 300 K by coupling it to a thermal bath.[51]

The dynamics were run for 50 ps (variable temperature) or 200 ps (constant temperature), the trajectory was sampled by minimising and storing the structure every picosecond.

References

1 J. C. Gasc and A. Bryskier, *Macrolides*, ed. A. Bryskier, J. Butzler, H. Neu and P. Tulkens, Arnette Blackwell, Oxford, 1993, vol. 47, pp. 5–66.
2 H. A. Kirst and G. D. Sides, *Antimicrob. Agents Chemother.*, 1989, **33**, 1413.
3 D. Mansuy and M. Delaforge, *Macrolides*, ed. A. Bryskier, J. Butzler, H. Neu and P. Tulkens, Arnette Blackwell, Oxford, 1993, pp. 635–646.
4 T. Cachet, G. Van den Mooter, R. Hauchecorne, C. Vinckier and J. Hoogmartens, *Int. J. Pharm.*, 1989, **55**, 59.
5 M. Skinner, R. B. Taylor and I. Kanfer, *Eur. J. Pharm. Sci.*, 1993, **1**, 61.
6 T. Watanabe, T. Fujii, H. Sakurai, J. Abe and K. Satake, *International Symposium on the Chemistry of Natural Products*, Kyoto, 1964, 146.
7 S. Omura, H. Ogura and T. Hata, *Tetrahedron Lett.*, 1967, 1267.
8 M. Hiramatsu, A. Furusaki, T. Noda, K. Naya, Y. Tomiie, I. Nitta, T. Watanabe, T. Take, J. Abe, S. Omura and T. Hata, *Bull. Chem. Soc. Jpn.*, 1970, **43**, 1966.
9 G. Bertho, P. Ladam, J. Gharbi-Benarous, M. Delaforge and J. P. Girault, *J. Chim. Phys.*, 1998, **95**, 423.
10 G. Bertho, J. Gharbi-Benarous, P. Ladam, M. Delaforge and J. P. Girault, *Bioorg. Med. Chem.*, 1998, **6**, 209.
11 R. C. Goldman, S. W. Fesik and C. C. Doran, *Antimicrob. Agents Chemother.*, 1990, **34**, 426.
12 R. Fernandez-Munoz and D. Vazquez, *J. Antibiot.*, 1973, **26**, 107.
13 S. Pestka, *Antimicrob. Agents Chemother.*, 1974, **6**, 474.
14 J. Barber, J. I. Gyi and D. A. Pye, *J. Chem. Soc.*, *Chem. Commun.*, 1991, 1249.
15 D. A. Pye, J. I. Gyi and J. Barber, *J. Chem. Soc.*, *Chem. Commun.*, 1990, 1143.
16 J. I. Gyi, R. J. Brennan, D. A. Pye and J. Barber, *J. Chem. Soc.*, *Chem. Commun.*, 1991, 1471.
17 G. Dinos, D. Synetos and C. Coutsogeorgopoulos, *Biochemistry*, 1993, **32**, 10638.
18 D. J. Hardy, D. M. Hensey, J. M. Beyer, C. Vojtko, E. J. McDonald and P. B. Fernandes, 1988, **32**, 1710.
19 E. Sartori, M. Delaforge and D. Mansuy, *Biochem. Pharmacol.*, 1989, **38**, 2061.
20 M. Delaforge and E. Sartori, *Biochem. Pharmacol.*, 1990, **40**, 223.
21 J. C. Gasc and A. Bryskier, *Macrolides*, ed. A. Bryskier, J. Butzler, H. Neu and P. Tulkens, Arnette Blackwell, Oxford, 1993, vol. 47, pp. 67–69.
22 M. Delaforge, M. Jaouen and D. Mansuy, *Biochem. Pharmacol.*, 1983, **32**, 2309.
23 S. Omura and M. Tishler, *J. Med. Chem.*, 1972, **15**, 1011.
24 C. Agouridas, P. Collette, P. Mauvais and J. F. Chantot, *34th Interscience Conference on Antimicrobial Agents and Chemotherapy, DC*, American Society for Microbiology, 1994, F-166.
25 M. R. Bendall and D. T. Pegg, *J. Magn. Reson.*, 1983, **53**, 272.
26 A. Bax and M. F. Summers, *J. Am. Chem. Soc.*, 1986, **108**, 2093.
27 A. Rutar, *J. Magn. Reson.*, 1984, **59**, 306.
28 A. Bax and R. Freeman, *J. Magn. Reson.*, 1981, **44**, 542.
29 T. C. Wong and V. Rutar, *J. Am. Chem. Soc.*, 1984, **106**, 7380.

30 A. Bax, *J. Magn. Reson.*, 1984, **57**, 314.
31 J. Gharbi-Benarous, M. Delaforge, C. K. Jankowski and J. P. Girault, *J. Med. Chem.*, 1991, **34**, 1117.
32 P. Ladam, J. Gharbi-Benarous, M. Piotto, M. Delaforge and J. P. Girault, *Magn. Reson. Chem.*, 1994, **32**, 1.
33 C. A. G. Haasnoot, F. De Leeuw and C. Altona, *Tetrahedron*, 1980, **36**, 2783.
34 I. Tvaroska, M. Hricovini and E. Petrakova, *Carbohydr. Res.*, 1989, **189**, 359.
35 J. R. Everett, I. K. Hatton and J. W. Tyler, *Magn. Reson. Chem.*, 1990, **28**, 114.
36 J. Gharbi-Benarous, P. Ladam, M. Delaforge and J. P. Girault, *J. Chem. Soc.*, *Perkin Trans. 2*, 1993, 2303.
37 P. Dauber-Osguthorpe, V. A. Roberts, D. J. Osguthorpe, J. Wolff, M. Genest and A. T. Hagler, *Proteins: Struct., Funct. Genet.*, 1988, **4**, 31.
38 S. J. Weiner, P. Kollmann, D. A. Case, U. C. Singh, C. Ghio, G. Alagona, S. Profeta and P. Weiner, *J. Am. Chem. Soc.*, 1984, **106**, 765.
39 N. R. Nirmala, G. M. Lippens and K. Hallenga, *J. Magn. Reson.*, 1992, **100**, 25.
40 P. Alam, J. Barber, R. J. Brennan, K. Kennedy and M. H. H. Tehrani, *Magn. Reson. Chem.*, 1995, **33**, 228.
41 G. Bertho, P. Ladam, J. Gharbi-Benarous, M. Delaforge and J. P. Girault, *Int. J. Biol. Macromol.*, 1998, **22**, 103.
42 K. Osono, K. Moriyama and M. Murakami, *J. Antibiot.*, 1974, **27**, 366.
43 T. R. Tritton, *Biochemistry*, 1977, **16**, 4133.
44 A. Awan, R. J. Brennan, A. C. Regan and J. Barber, *J. Chem. Soc.*, *Chem. Commun.*, 1995, **16**, 1653.
45 H. E. Homann and K. H. Nierhaus, *Eur. J. Biochem.*, 1971, **20**, 249.
46 D. Vazquez, *Inhibitors of Protein Synthesis*, Springer Verlag, Berlin, 1979.
47 D. Moazed and H. F. Noller, *Biochimie*, 1987, **69**, 879.
48 A. Contreras and D. Vazquez, *Eur. J. Biochem.*, 1977, **74**, 539.
49 O. Bischof, H. Urlaub, V. Kruft and B. Wittmann-Liebold, *J. Biol. Chem.*, 1995, **270**, 23060.
50 U. Dinur and A. T. Hagler, *J. Chem. Phys.*, 1989, **91**, 2949.
51 H. J. C. Berendsen, J. P. M. Postma, W. F. v. Gunsteren, A. DiNola and J. R. Haak, *J. Chem. Phys.*, 1984, **81**, 3684.

Paper 8/08309F